Time reversing solitary waves

Jean-Pierre Fouque
Department of Mathematics, North Carolina State University, Raleigh NC 27695-8205.

Josselin Garnier
Laboratoire de Statistique et Probabilités, Université Paul Sabatier, 118 Route de Narbonne, 31062 Toulouse Cedex 4, France.

Juan Carlos Muñoz Grajales
Departamento de Matemáticas, Universidad del Valle, Cali, Colombia.

André Nachbin
Instituto de Matemática Pura e Aplicada, Est. D Castorina 110, Jardim Botânico, Rio de Janeiro, RJ 22460-320, Brazil (author for correspondence).

(Dated: December 8, 2003)

We present new results for the time reversal of nonlinear pulses traveling in a random medium, in particular for solitary waves. We consider long water waves propagating in the presence of a spatially random depth. Both hyperbolic and dispersive regimes are considered. We demonstrate that in the presence of properly scaled stochastic forcing the solution to the nonlinear (shallow water) conservation law is regularized leading to a viscous shock profile. This enables time-reversal experiments beyond the critical time for shock formation. Furthermore we present numerical experiments for the time reversed refocusing of solitary waves in a regime where theory is not yet available. Solitary wave refocusing simulations are performed with a new Boussinesq model, both in transmission and in reflection.

PACS numbers: 47.35.+i,42.25.Dd,43.25.Ts,43.60.Cg

Time-reversal refocusing for linear waves propagating in inhomogeneous media has been extensively studied in various contexts, as for example in ultrasound and underwater acoustics [1]. Applications include telecommunication [2] and imaging [3]. From the mathematical point of view, a first proof of one-dimensional time-reversal refocusing in reflection has been obtained by Clouet and Fouque [4]. In this Letter we consider one-dimensional nonlinear waves and the benefits of randomness as a regularizing mechanism. Namely, under stochastic forcing the transmitted nonlinear pulse is governed, to leading order, by a viscous Burgers equation where the "apparent viscosity" depends on statistical properties of the random medium. This is the first time where this result is presented. We also consider waves in the dispersive regime. In this case time-reversal recompresses the deterministic oscillatory (Airy-like) tail behind the wavefront, along with the incoherent forward scattered signal. As a consequence of these two results we are able to show numerically, also for the first time, the time-reversal refocusing of solitary waves. The theoretical results for the time reversal of linear dispersive waves and for the time-reversal of nonlinear hyperbolic waves are briefly described below. A detailed version of these theories will be presented in future publications. Moreover, no theory is yet available for the time-reversal of weakly dispersive, weakly nonlinear solitary waves.

Recently a terrain-following Bousssinesq system [5] has been formulated for the propagation of long water waves over highly disordered topographies. This system is in the form

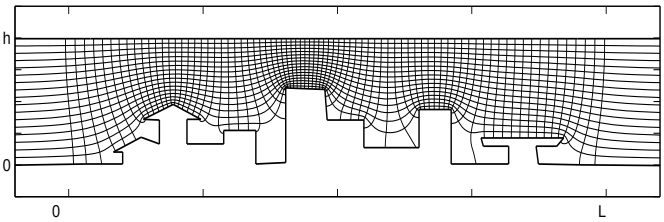

FIG. 1: Terrain-following (curvilinear) coordinate system.

$$M(\xi)\eta_t + \left(\left[1 + \alpha\eta/M(\xi)\right] U \right)_\xi = 0,$$
$$U_t + \eta_\xi + 0.5\alpha \left(u^2/M(\xi)^2\right)_\xi = \beta/3\, U_{\xi\xi t}$$

where η is the free surface elevation and U is the depth-averaged terrain-following velocity component. The characteristic wave amplitude is a_o, the characteristic wavelength is λ and the typical depth is h_o. The nonlinearity parameter is $\alpha = a_o/h_o$ and the dispersion parameter is $\beta = (h_o/\lambda)^2$. The metric term $M(\xi)$ is defined by $M(\xi) \equiv \tilde{y}_{\tilde{\zeta}}(\xi, 0)$, $\tilde{y} \equiv \beta^{1/2} y$, where curvilinear coordinates $(\xi, \tilde{\zeta})$ are used over the depth as indicated in Fig. 1. The disordered topography is not restricted to being a graph of a function. In the absence of a topography this system reduces to the usual dimensionless Boussinesq system [6]. Solitary wave profiles can be cal-

culated by using the corresponding second order Boussinesq equation [7]. These are approximate traveling wave solutions to the Boussinesq system. Nevertheless they behave as traveling waves for a wide parameter range [7]. In this Letter the results are focused on time-reversal in transmission. In both cases the integral of the autocorrelation function of the fluctuations controls the level of coherent energy converted into incoherent energy for both forward and back scattered signals. Stronger fluctuations will increase the refocused amplitude in reflection and therefore decrease the refocused amplitude in transmission [4]. Usually the theoretical analysis is carried out in two asymptotic frameworks: i) the *weak fluctuations* regime, in which the medium's correlation length and the typical wavelength are on the same scale; ii) the *strong fluctuations* regime, where the correlation length is smaller than the typical wavelength. The fluctuation amplitude is scaled by a small (case i) or order one (case ii) parameter. But some ambiguity can always be left through a constant factor multiplying the small parameter. Our presentation is broken into three topics. We plan to publish the details elsewhere, with one article for each topic. The first topic has been submitted for publication [8]. In these future papers we will also present results for time-reversal in reflection.

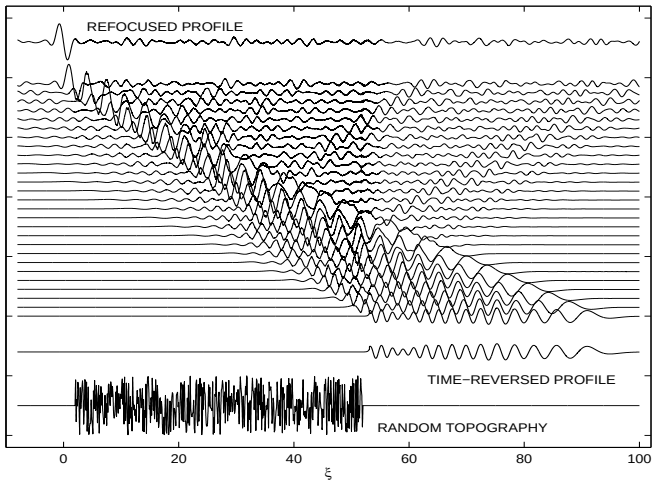

FIG. 2: Time-reversal in transmission for a dispersive ($\beta = 0.1$) pulse $\eta_o(x) = -10x\exp(-x^2/0.08)$. The random topography fluctuations are sampled at mesh points and connected by straight lines. The fluctuation level is 50% of the total depth. The correlation length is 10% of the effective pulse width. The dynamics is described in the vertical direction of the graph. The initial and final configurations have been displayed separately from the evolution set.

Dispersive time-reversal [8]: Consider the linearized version of the terrain-following Boussinesq system. The random medium (i.e. topography) is absorbed in the metric term $M(\xi)$ through the change of coordinate system. The time-reversal theory for linear dispersive waves makes use of the right and left dispersive propagating modes which are coupled due to the presence of a random medium. The dispersive time-reversal results can then be described as follows: a long pulse shaped wave is sent through a highly fluctuating, rapidly varying random medium. The transmitted pulse front undergoes a great transformation due to apparent diffusion (promoted by the random medium) and the oscillatory phase lag (promoted by dispersion). A particularly interesting property along the transmitted pulse front is that its effective dispersion decreases due to the random medium in the sense that the dispersive tail is reduced due to the backscattering of the high frequencies. The two mechanisms above are captured mathematically by the composition of two convolutions with the transmitted mode: one has a Gaussian kernel representing the apparent diffusion mechanism and the other has an Airy kernel capturing the dispersion. Behind the pulse front we can observe a coda consisting of incoherent fluctuations due to multiple scattering. The total transmitted energy decays exponentially with the propagation distance due to Anderson localization [8]. The transmitted signal, including both the coherent pulse front and the incoherent coda, is recorded, time-reversed and sent back in the opposite direction from which it came. See the bottom trace in Fig. 2. Under time-reversion both the incoherent and deterministic oscillations are recompressed at the original source location as seen at the top of Fig. 2. Dispersive time-reversal recompression of the Airy function in a homogeneous medium has been first observed in [9]. Statistical stability is observed even in the presence of dispersion. Dispersion provides an improvement for source location, in one-dimension, as a consequence of the recompression of the dispersive tail which in the time-reversal experiment is ahead of the pulse. As soon as the recompressed pulse travels over the original source location a dispersive oscillatory tail starts to develop behind the pulse. The source location is precisely where there is no dispersive oscillation; neither in front nor behind the pulse. Time reversal experiments in reflection have also been performed and one can clearly see incoherence being recompressed first followed by the dispersive recompression.

Nonlinear time-reversal: The time-reversal theory for nonlinear acoustic waves has been investigated experimentally by Tanter *et al.* [10]. They analyzed the nonlinear mechanism for energy transfer to higher harmonic components during forward propagation. The main goal of their experiments was to check for the reversibility of this energy transfer. The acoustic experiments were carried out for a nonlinear sinusoidal wave propagating in a homogeneous medium. The energy reversibility among harmonics is broken only for propagation longer than the shock formation distance. We address this issue for a broadband pulse in the presence of randomness. We show, for the first time, how the random medium regularizes the problem allowing for propagation beyond

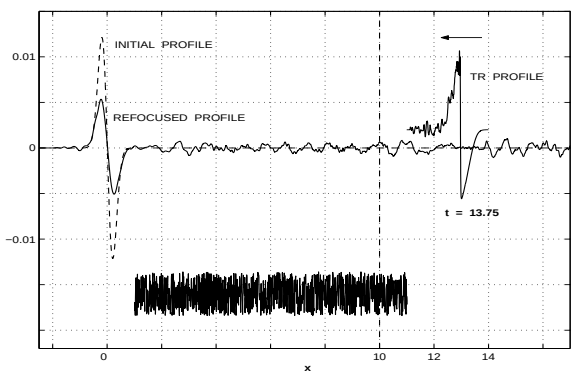

FIG. 3: Time-reversal in transmission for a nonlinear hyperbolic ($\alpha = 0.01$) pulse. The critical time (computed from Burgers equation) is $t_c = -1/(\alpha\eta_o') = 1/(10\alpha)$. The initial (unit width) wave profile $\eta_o(x)$ considered is the derivative of a Gaussian. The random topography fluctuations (with $\varepsilon = 0.6$) is of the same type as in the dispersive simulation. The time-reversed data (recorded beyond the shock distance) has been slightly lifted for better display.

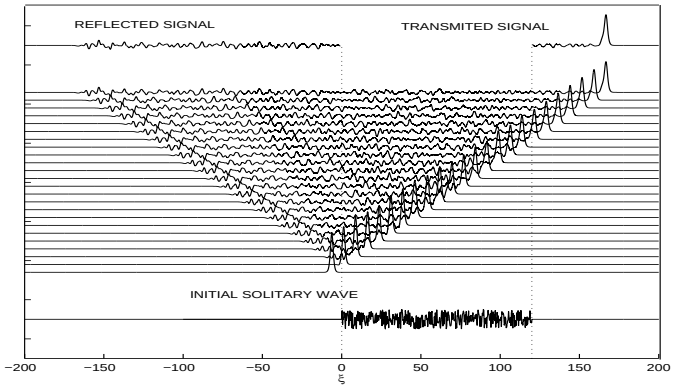

FIG. 4: Forward propagation of a solitary wave, as indicated by the bottom trace. The dynamics is described in the vertical direction of the graph. The recorded reflected and transmitted signals are presented at the top. The parameters are $\alpha = \beta = 0.01$ and the fluctuation level is 50% of the total depth.

the shock distance. Just as in the super-resolution case [11], this is another instance where randomness helps in a dramatic fashion. The description of the mathematical theory is as follows. The time-reversal theory for nonlinear hyperbolic waves makes use of the right and left Riemann invariants $A(x,t) = (\alpha u - 2c + 2)/\alpha$ and $B(x,t) = (\alpha u + 2c - 2)/\alpha$, corresponding to the underlying ($\varepsilon = 0$) nonlinear shallow water system which arises from [12]

$$\eta_t + ((1 + \varepsilon h + \alpha\eta)u)_x = 0,$$
$$u_t + \eta_x + \alpha u u_x = 0.$$

The local propagation speed is $c = \sqrt{1+\alpha\eta}$, where now u is the horizontal depth-averaged velocity component. The random fluid body is given by $H(x,t) = 1 + \varepsilon h(x) + \alpha\eta(x,t)$, where $-h(x)$ denotes the disordered topography. This shallow water system is rewritten in terms of these undisturbed Riemann invariants. In the presence of stochastic forcing they are not invariant along characteristics, being actually coupled due to the random scattering. Using a convenient set of changes of variables the Riemann invariant system is written as a triangular (two-by-two) system of partial differential equations. The equation for the leading order transmitted quantity is integrated over the corresponding characteristic thus enabling the use of a limit theorem for ordinary differential equations with a stochastic right hand side [13]. It follows that the transmitted pulse front is (to leading order) governed by a viscous Burgers equation. The apparent viscosity reads as a pseudo-differential operator imposed by the power spectral density of the random fluctuations. The apparent viscosity does not remove energy from the system. It only converts coherent wave energy into incoherent fluctuations. In the linear regime this mechanism leads to pulse spreading and attenuation. In the nonlinear regime it is well known [6] that for a viscous Burgers equation a shock structure will develop on a scale controlled by the nonlinearity and the apparent viscosity. Having prevented a derivative singularity from emerging, the fast transition layer saturates (i.e. the shock structure forms) and a self-similar traveling wave may emerge from the balance between nonlinearity and the stochastic forcing [6, Section 4.3]. This combined mechanism is enough to prevent the shock from fully developing and therefore it allows for the propagation beyond the shock distance. Hence time-reversal can be performed beyond the critical time. A time-reversal in transmission result is presented in Fig. 3. We were also able to capture the time-reversal of a pulse in a homogeneous medium and to provide numerical evidence of the complete inverse cascading of energy from the harmonics produced by nonlinearity. This is in agreement with the single harmonic experiment performed by Tanter *et al.* [10]. In a random environment the refocused pulse, for time-reversal in transmission, contains only part of the energy (c.f. Fig. 3) since the reflected energy is not considered in the recompression. As the fluctuation level increases even more reflection is generated and less energy will be recompressed in transmission. We believe that these results should apply to other nonlinear conservation laws. In particular for those systems which support Riemann invariants. One application is gas dynamics. A trivial example is the case of a polytropic gas with adiabatic exponent equal to 2. It is well known that this model is analogous to the shallow water system presented above [6].

Time-reversing solitary waves: Having fully understood the roles played by dispersion and by nonlinearity we are in a position to present for the first time the time-reversal of solitary waves. For the terrain-

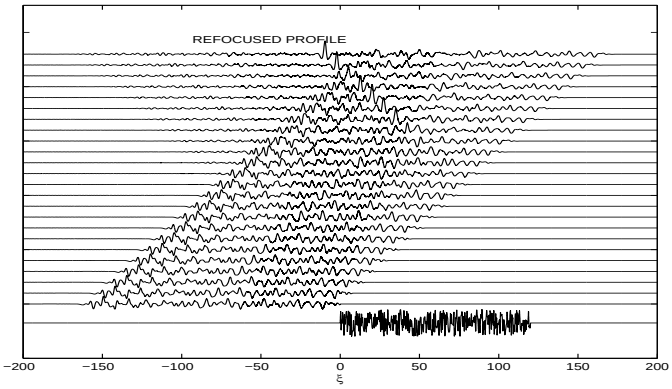

FIG. 5: Time-reversal experiment for the reflected signal generated by a solitary wave as described in Fig. 4.

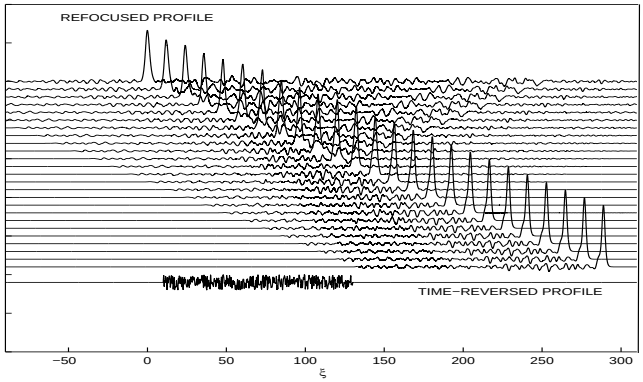

FIG. 6: Time-reversal experiment for the transmitted signal generated by a solitary wave as described in Fig. 4. The recording time is longer than in Fig. 4 and therefore the random topography was shifted to the left of the computational domain.

following Boussinesq system these waves are of the form $\eta(\xi,0) = A_1\ \mathrm{sech}^2(B(\xi-\xi_o)) + A_2\ \mathrm{sech}^4(B(\xi-\xi_o))$, $U(\xi,0) = A\ \mathrm{sech}^2(B(\xi-\xi_o))$, with $A_1(\alpha)$, $A_2(\alpha)$, $A(\alpha)$ and $B(\alpha)$ constants [7]. These are approximate solutions to the Boussinesq system with $M \equiv 1$ (see [7]). Time-reversal experiments are performed both in transmission and in reflection. In either case a signal is recorded at the corresponding end of the disordered channel, time-reversed, and sent back into the random medium (c.f. Fig. 4). The striking time-reversed refocusing of the solitary wave is observed in both cases, in particular for time reversal in reflection where the back scattered incoherent signal is not very intense. For time-reversal in reflection (Fig. 5) a coherent (refocused) pulse emerges from the recompression of the weak back scattered incoherent signal at exactly the position where the initial solitary wave was placed ($\xi = -10$). The refocusing time is equal to the length of the time interval used to record the reflected signal, indicated at the top of Fig. 4. This small travelling wave propagates to the left, into the homogeneous section of the channel. The time-reversal experiment in transmission is presented in Fig. 6. We recorded the transmitted wave for a longer interval than presented at the top of Fig. 4. As in linear hyperbolic problems the coda needs to be long enough in order for recompression take place in the back propagation. Hence the longer time-reversed signal is presented at the bottom (right) of Fig. 6. Noise recompression can be seen at the front of the solitary wave but in a weaker form when compared to previous regimes. For the transmitted wave it is also very interesting to observe, in some cases, the mild steepening of the solitary wave at the pulse front. This is due to the decrease of the effective dispersion as mentioned earlier. The lack of balance between nonlinearity and the effective dispersion promotes the slow steepening at the front. This is at a much slower rate than in the hyperbolic case due to dispersion. Moreover statistical stability is still observed for the refocused pulse both in transmission as well as in reflection.

We have presented in this paper the striking time-reversed refocusing of solitary waves, both in transmission and in reflection. Even though a theory is not readily available for weakly dispersive, weakly nonlinear solitary waves, we have described the new theories for linear dispersive time-reversal as well as nonlinear hyperbolic time-reversal. It would be very interesting to obtain a weakly dispersive, weakly nonlinear theory and to explore the connection with other physical models which support solitons.

[1] M. Fink, Scientific American, November, p. 67 (1999).
[2] A. Derode, A. Tourin, J. de Rosny, M. Tanter, S. Yon, and M. Fink, Phys. Rev. Lett. **90**, 014301 (2003).
[3] M. Fink, G. Montaldo, and M. Tanter, Ann. Rev. Biomedical Eng. **5**, 465 (2003).
[4] J.-F. Clouet and J.-P. Fouque, Wave Motion **25**, 361 (1997).
[5] A. Nachbin, SIAM J. Appl. Math. **63**, 905 (2003).
[6] G. Whitham, *Linear and Nonlinear Waves* (John Wiley, New York, 1974).
[7] G. Wei and J. Kirby, J. Waterway, Port, Coastal and Ocean Eng. **121**, 251 (1995).
[8] J.-P. Fouque, J. Garnier, and A. Nachbin, SIAM J. Appl. Math. p. submitted (2003).
[9] E. Pelinovskya, T. Talipova, and C. Kharif, Physica D **147**, 83 (2000).
[10] M. Tanter, J. Thomas, F. Coulouvrat, and M. Fink, Phys. Rev. E **64**, 016602 (2001).
[11] P. Blomgren, G. Papanicolaou, and H. Zhao, JASA **111**, 230 (2002).
[12] L. Debnath, *Nonlinear Partial Differential Equations for Scientists and Engineers* (Birkhäuser, Boston, 1997).
[13] R. Khasminskii, Theory Probab. Appl. **11**, 390 (1966).